

Adaptive Control for a Non-minimum Phase Hypersonic Vehicle Model

YE Linqi¹, ZONG Qun¹, ZHANG Xiuyun¹

1. Department of Electrical Engineering and Automation, Tianjin University, Tianjin 300072, China
E-mail: yelinqi@tju.edu.cn

Abstract: A non-minimum phase hypersonic vehicle model is used as control model in this paper, simultaneously a new control-oriented model is developed to solve the non-minimum phase problem. By properly neglecting or treating some items as uncertainties, a simpler control-oriented model is presented. In the new control-oriented model, the altitude loop is approximately an integral chain, thus backstepping method can be conveniently used. The uncertainty in the model is estimated by adaptive method and the adaptive law is designed by Lyapunov theory to guarantee the stability of the whole system. The simulation results validate the effectiveness of the methodology and a monte-carlo test is carried to illustrate the robustness of this method.

Key Words: Hypersonic vehicle, Non-minimum phase, Control-oriented model, Adaptive Control, Backstepping

1 Introduction

Hypersonic vehicle, which refers to vehicle that can fly in atmosphere at the speed of more than five times the speed of sound, has received more and more attention from countries around the world in recent years. The success of X-43A opens the door of air-breathing hypersonic vehicle which is powered by scramjet engine and has integrated configuration^[1-2]. Due to the coupling between the propulsion system and the aerodynamics, and elastic effects caused by slender body as well as impact of shock wave and aero-thermal effects, it becomes a big challenge to design control system for hypersonic vehicle.

As a prior work of control design, many researchers have studied the modeling of air-breathing hypersonic vehicle^[3-5]. Reference [3] developed flexible air-breathing hypersonic vehicle model by approximating forces and moments by the least squares method. Besides, reference [3] also simplified the model to obtain a feedback linearization model, which was so-called "control-oriented model". Unlike reference [3], reference [4] introduced deflections of the forebody turn angle and aftbody vertex angle to represent the interactions between flexible mode and rigid body. Based on reference [3], reference [5] extended the influence of flexible mode to all forces and moments and obtained a more accurate model.

Reference [5] analyzed the zero-dynamics in hypersonic vehicle model, pointed that hypersonic vehicle model exhibit non-minimum phase when choosing velocity and altitude as outputs, which was caused by the coupling from elevator to lift. That is to say, the internal dynamics will be unstable when using traditional standard inversion methods. To ensure the stability of internal dynamics, an usual way is control-oriented modeling^[3]. In reference [3], elevator in lift is neglected to raise the relative degree of altitude. Thus the original model can be stabilized by the controller developed by the control-oriented model. The simplification certainly will cause uncertainties from the original model, so adaptive control is usually used to overcome the uncertainties. Many

literatures have proposed controller for the control-oriented model in reference [3]. The most widely used method is feedback linearization and backstepping.

As to feedback linearization method, there are mainly two ways to go on. One is using linear methods for feedback linearization model. References [3] and [6-8] proposed linear quadratic regulator (LQR) controller using static or dynamic feedback, deciding the optimal feedback coefficients by minimizing the performance-cost function, while reference [9] used H_∞ method to determine feedback coefficients by solving Linear Matrix Inequality(LMI). Another way is using high order sliding mode control^[10-13]. Firstly a high order sliding surface containing output and its derivatives of various orders is designed, thus the input appeared in the first derivative of sliding surface. Then the input is obtained by using reaching law to guarantee the sliding surface be reached in finite time. Once the sliding surface is reached, the output tracking error will converge to zero.

When using backstepping method, system is usually divided into two subsystems: the velocity loop and the altitude loop. The velocity loop is only first-order, so the control law of fuel equivalence ratio can be obtained by dynamic inversion. As the altitude loop is fourth-order, backstepping is used to design virtual input one by one until obtaining the elevator control law. According to the techniques used in backstepping, methods such as filter backstepping and dynamic surface are derived. References [14-15] use backstepping for altitude loop, where flight path angle was considered as output and integral extension was used for flight path angle. In order to avoid the trouble of calculating derivative of virtual input, reference [16] introduced two integral filters in each step to estimate the derivative of virtual input. Similarly, reference [17] used dynamic surface method, which estimated the derivative of virtual input by a one order filter. Reference [18] followed the idea of dynamic surface, and used neural network to replace the uncertain nonlinear function in the model. On the basis of reference [18], reference [19] further introduced an additional subsystem to handle the problem of input constraints.

In summary, many control methods have been proposed for hypersonic vehicle. But when using feedback

*This work is supported by National Natural Science Foundation (NNSF) of China under Grant 61273092, 61203012, Science and Technology Development Fund of Tianjin Colleges and Universities under Grant 20140817.

linearization method, it requires to calculate the analytical expression of higher order derivatives of outputs, which is quite complex. And backstepping methods are usually based on the control-oriented model in reference [3], which will meet trouble when calculating the derivative of virtual input because the model is not strict feedback form. So researchers usually add filter to estimate the derivative of virtual input, of course, which makes the design more complex. In this paper, a simpler control-oriented model is developed by properly neglecting or treating some items as uncertainty. In the new control-oriented model, the altitude loop is approximately an integral chain, thus backstepping method can be conveniently used. The uncertainty in the model is estimated by adaptive method and the adaptive law is designed by Lyapunov theory to guarantee the stability of the whole system.

2 Model Introduction

In this paper, the flexible model of air-breathing hypersonic vehicle with non-minimum phase developed in reference [5] is used as simulation model, which is described as equation (1).

$$\begin{aligned} m\dot{V} &= T \cos \alpha - D - mg \sin \gamma \\ \dot{h} &= V \sin \gamma \\ \dot{\gamma} &= \frac{L + T \sin \alpha}{mV} - \frac{g}{V} \cos \gamma \\ \dot{\theta} &= Q \\ I_{yy} \dot{Q} &= M \\ \ddot{\eta}_i &= -2\zeta_i \omega_i \dot{\eta}_i - \omega_i^2 \eta_i + N_i, \quad i = 1, 2, 3. \end{aligned} \quad (1)$$

Reference [20] has given the value of ω_i at different fuel levels as shown in table 1, the value at 50% fuel level is chosen as nominal value in later simulation.

Table 1: Modal frequencies at different fuel levels

Fuel Level	0%	30%	50%	70%	100%
m(slug)	93.57	126.1	147.9	169.6	202.2
ω_1 (rad/s)	22.78	21.71	21.17	20.73	20.17
ω_2 (rad/s)	68.94	57.77	53.92	51.24	48.4
ω_3 (rad/s)	140	117.8	109.1	102.7	95.6

The forces and moments are functions of states and inputs, as formula (2).

$$\begin{aligned} T &= \bar{q}S [C_{T,\phi} \phi + C_T + C_T^\eta \eta], L = \bar{q}SC_L, D = \bar{q}SC_D, M = z_T T + \bar{q}cSC_M \\ N_i &= \bar{q}S [N_i^{\alpha^2} \alpha^2 + N_i^\alpha \alpha + N_i^{\delta_e} \delta_e + N_i^0 + N_i^\eta \eta], \quad i = 1, 2, 3 \end{aligned} \quad (2)$$

Where

$$\begin{aligned} C_{T,\phi} &= C_T^{\phi\alpha^3} \alpha^3 + C_T^{\phi\alpha^2} \alpha^2 + C_T^{\phi\alpha} \alpha + C_T^\phi \\ C_T &= C_T^{\alpha^3} \alpha^3 + C_T^{\alpha^2} \alpha^2 + C_T^\alpha \alpha + C_T^0 \\ C_M &= C_M^{\alpha^2} \alpha^2 + C_M^\alpha \alpha + C_M^{\delta_e} \delta_e + C_M^0 + C_M^\eta \eta \\ C_L &= C_L^\alpha \alpha + C_L^{\delta_e} \delta_e + C_L^0 + C_L^\eta \eta \\ C_D &= C_D^{\alpha^2} \alpha^2 + C_D^\alpha \alpha + C_D^{\delta_e^2} \delta_e^2 + C_D^{\delta_e} \delta_e + C_D^0 + C_D^\eta \eta \\ C_j^\eta &= [C_j^{\eta_1} \quad 0 \quad C_j^{\eta_2} \quad 0 \quad C_j^{\eta_3} \quad 0], \quad j = T, M, L, D \\ N_i^\eta &= [N_i^{\eta_1} \quad 0 \quad N_i^{\eta_2} \quad 0 \quad N_i^{\eta_3} \quad 0], \quad i = 1, 2, 3. \end{aligned} \quad (3)$$

Where \bar{q} is dynamic pressure defined as formula (4)

$$\bar{q} = \frac{\rho V^2}{2} \quad (4)$$

and the approximation (5)

$$\rho \approx \rho_0 e^{-(h-h_0)/h_s} \quad (5)$$

is used here. The value of all coefficients can be found in reference [5] and are shown in table 2, table 3 and table 4.

Table 2: Vehicle Parameters

Notation	Meaning	Value	Unit
g	Acceleration due to gravity	32.17	ft/s ²
I_{yy}	Moment of inertia	86722.54	slug*ft ² /rad
S	Reference area	17	ft ²
\bar{c}	Mean aerodynamic chord	17	ft
z_T	Thrust-to-moment coupling coefficient	8.36	ft
ρ_0	Air density at nominal altitude	6.7429e-5	slugs/ft ³
h_s	Inverse of the air density exponential decay rate	21358.8	ft
h_0	Nominal altitude	85000	ft

Table 3: Aerodynamic Parameters

Mark	Value	Unit	Mark	Value	Unit
C_L^α	5.9598	rad ⁻¹	C_M^0	0.16277	
$C_L^{\delta_e}$	0.73408	rad ⁻¹	$C_M^{\delta_e}$	-1.3642	rad ⁻¹
C_L^0	-0.024377		$C_M^{\eta_1}$	-0.0071776	ft ⁻¹
$C_L^{\eta_1}$	-0.034102	ft ⁻¹	$C_M^{\eta_2}$	-0.030220	ft ⁻¹
$C_L^{\eta_2}$	-0.031737	ft ⁻¹	$C_M^{\eta_3}$	-0.010666	ft ⁻¹
$C_L^{\eta_3}$	-0.067580	ft ⁻¹	$C_T^{\phi\alpha^3}$	-14.038	rad ⁻³
$C_D^{\alpha^2}$	7.9641	rad ⁻²	$C_T^{\phi\alpha^2}$	-1.5839	rad ⁻¹
C_D^α	-0.074020	rad ⁻¹	$C_T^{\phi\alpha}$	0.69341	rad ⁻¹
$C_D^{\delta_e^2}$	0.91021	rad ⁻²	C_T^ϕ	0.19904	
$C_D^{\delta_e}$	1.0840*10 ⁻⁶	rad ⁻¹	C_T^3	1.0929	rad ⁻³
C_D^0	-0.019880	rad ⁻²	C_T^2	0.97141	rad ⁻¹
$C_D^{\eta_1}$	0.0012934	rad ⁻¹	C_T^1	0.037275	rad ⁻¹
$C_D^{\eta_2}$	0.00025523		C_T^0	-0.021635	
$C_D^{\eta_3}$	0.0027066	ft ⁻¹	$C_T^{\eta_1}$	-0.0027609	ft ⁻¹
$C_M^{\alpha^2}$	6.8888	ft ⁻¹	$C_T^{\eta_2}$	-0.0034979	ft ⁻¹
C_M^α	5.1390	ft ⁻¹	$C_T^{\eta_3}$	-0.0053310	ft ⁻¹

Table 4: Coefficients of generalized forces

Mark	Value	Mark	Value	Mark	Value
$N_1^{\alpha^2}$	-0.089274	$N_2^{\alpha^2}$	8.8374e-2	$N_3^{\alpha^2}$	-7.4826e-2
N_1^α	0.34971	N_2^α	9.5685e-2	N_3^α	0.10299
N_1^0	2.7562e-3	N_2^0	1.3834e-3	N_3^0	-1.9277e-3
$N_1^{\delta_e}$	0.039029	$N_2^{\delta_e}$	-2.4875e-2	$N_3^{\delta_e}$	-4.2624e-3
$N_1^{\eta_1}$	-9.3415e-4	$N_2^{\eta_1}$	4.1120e-4	$N_3^{\eta_1}$	3.2963e-4
$N_1^{\eta_2}$	-6.7015e-4	$N_2^{\eta_2}$	1.0924e-4	$N_3^{\eta_2}$	3.0022e-4
$N_1^{\eta_3}$	-1.8813e-3	$N_2^{\eta_3}$	8.5621e-4	$N_3^{\eta_3}$	6.5423e-4

Because of the coupling from elevator to lift, δ_e appears in $\dot{\gamma}$. Standard inversion method obtains the control law of δ_e by taking inversion of the dynamics of \dot{h} and $\dot{\gamma}$, which makes the internal dynamics $\dot{\theta}$ and \dot{Q} unstable. To deal with this problem, we can treat δ_e in $\dot{\gamma}$ as uncertainty to raise the relative degree of h so that δ_e in altitude loop only appears in \dot{Q} , then the control process naturally turns into $\delta_e \rightarrow Q \rightarrow \theta \rightarrow \gamma \rightarrow h$. Furthermore, to constitute an integral chain, all items except θ in $\dot{\gamma}$ are treated as uncertainties. Besides, to decouple velocity loop and altitude loop, δ_e in \dot{V} is regarded as uncertainty and ϕ in \dot{Q} is neglected. It will not cause steady-state error because h is directly controlled by γ , as long as the uncertainty in $\dot{\gamma}$ is compensated, h can be tracked exactly. Thus the control-oriented model is described as equation (6).

$$\begin{aligned} \dot{V} &= f_v + g_v \phi + \Delta_v \\ \dot{h} &= V\gamma \\ \dot{\gamma} &= \theta + \Delta_\gamma \\ \dot{\theta} &= Q \\ \dot{Q} &= f_q + g_q \delta_e \end{aligned} \quad (6)$$

Where

$$\begin{aligned} f_v &= \frac{\bar{q}SC_\tau \cos \alpha - D - mg \sin \gamma}{m} \\ g_v &= \frac{\bar{q}SC_{T,\phi} \cos \alpha}{m} \\ f_q &= \frac{z_r \bar{q}SC_\tau + \bar{q}cS(C_M^{\alpha^2} \alpha^2 + C_M^\alpha \alpha + C_M^0)}{I_{yy}} \\ g_q &= \frac{\bar{q}cSC_M^{\delta_e}}{I_{yy}} \end{aligned} \quad (7)$$

Δ_v and Δ_γ are uncertainties and the approximation $\sin \gamma \approx \gamma$ is used because γ is very small. $\tilde{\gamma}$ is defined as $\tilde{\gamma} = \gamma - \gamma_r$, where γ_r is the desired value of γ and is to be designed.

3 Control Design

3.1 Velocity Loop

Suppose the reference velocity is V_r , defining velocity tracking error as $\tilde{V} = V - V_r$ (Note: As a convention, letter with subscript r represents desired value of the state, and

letter with break line on its top means error between true value and desired value). Derivative of \tilde{V} is

$$\dot{\tilde{V}} = \dot{f}_v + g_v \phi + \Delta_v - \dot{V}_r \quad (8)$$

Let $\hat{\Delta}_v$ be an estimation of Δ_v and design ϕ as

$$\phi = g_v^{-1}(-k_v \tilde{V} - \dot{f}_v + \dot{V}_r - \hat{\Delta}_v) \quad (9)$$

Where $k_v > 0$. In what follows, if not explained the parameters are acquiescently positive number. Thus the closed loop of velocity turns into this form

$$\dot{\tilde{V}} = -k_v \tilde{V} + \Delta_v - \hat{\Delta}_v = -k_v \tilde{V} + \tilde{\delta}_v \quad (10)$$

Where $\tilde{\delta}_v = \Delta_v - \hat{\Delta}_v$ is the estimation error. Uncertainty Δ_v is viewed as a slow varying item so that $\dot{\Delta}_v \approx 0, \dot{\tilde{\delta}}_v = -\dot{\hat{\Delta}}_v$. And this idea will be used again later.

Select Lyapunov function

$$Y_v = \frac{1}{2} \tilde{V}^2 + \frac{1}{2b_v} \tilde{\delta}_v^2 \quad (11)$$

Take the derivative of Y_v

$$\begin{aligned} \dot{Y}_v &= \tilde{V} \dot{\tilde{V}} - \frac{1}{b_v} \tilde{\delta}_v \dot{\tilde{\delta}}_v \\ &= \tilde{V}(-k_v \tilde{V} + \tilde{\delta}_v) - \frac{1}{b_v} \tilde{\delta}_v \dot{\tilde{\delta}}_v \\ &= -k_v \tilde{V}^2 + \left(\tilde{V} - \frac{1}{b_v} \dot{\tilde{\delta}}_v \right) \tilde{\delta}_v \end{aligned} \quad (12)$$

Design adaptive law $\dot{\hat{\Delta}}_v = b_v \tilde{V}$, then $\dot{Y}_v = -k_v \tilde{V}^2 \leq 0$, so velocity loop is stable.

3.2 Altitude Loop

Altitude loop will use backstepping method. Unlike Δ_v , Δ_γ in the altitude loop is unmatched uncertainty^[21] and it need to be estimated for 3 times when using backstepping.

Firstly, design γ_r to make $h \rightarrow h_r$. Let

$$\gamma_r = (-k_h \tilde{h} + \dot{h}_r) / V \quad (13)$$

Then

$$\dot{\tilde{h}} = V(\gamma_r + \tilde{\gamma}) - \dot{h}_r = -k_h \tilde{h} + V\tilde{\gamma} \quad (14)$$

Select Lyapunov function

$$Y_h = \frac{1}{2} \tilde{h}^2 \quad (15)$$

Take the derivative of Y_h

$$\dot{Y}_h = \tilde{h} \dot{\tilde{h}} = -k_h \tilde{h}^2 + V\tilde{h}\tilde{\gamma} \quad (16)$$

As $\tilde{\gamma}$ will reach zero in the design process later, it can be written as $\dot{Y}_h \approx -k_h \tilde{h}^2$.

Secondly, design θ_r to make $\gamma \rightarrow \gamma_r$. Let

$$\theta_r = -k_\gamma \tilde{\gamma} - \dot{\hat{\Delta}}_1 \quad (17)$$

Then

$$\dot{\tilde{\gamma}} = \dot{\theta}_r + \dot{\tilde{\theta}} + \Delta_\gamma = -k_\gamma \tilde{\gamma} + \tilde{\theta} + \tilde{\delta}_1 \quad (18)$$

Select Lyapunov function

$$Y_\gamma = \frac{1}{2} \tilde{\gamma}^2 + \frac{1}{2b_\gamma} \tilde{\delta}_1^2 \quad (19)$$

Take the derivative of Y_γ

$$\begin{aligned}\dot{Y}_\gamma &= \tilde{\gamma}\dot{\tilde{\gamma}} + \frac{1}{b_\gamma}\tilde{\delta}_1\dot{\tilde{\delta}}_1 \\ &= \tilde{\gamma}\left(-k_\gamma\tilde{\gamma} + \tilde{\theta} + \tilde{\delta}_1\right) - \frac{1}{b_\gamma}\tilde{\delta}_1\dot{\tilde{\delta}}_1 \\ &= -k_\gamma\tilde{\gamma}^2 + \tilde{\gamma}\tilde{\theta} + \tilde{\delta}_1\left(\tilde{\gamma} - \frac{1}{b_\gamma}\dot{\tilde{\delta}}_1\right)\end{aligned}\quad (20)$$

Design adaptive law $\dot{\tilde{\delta}}_1 = b_\gamma\tilde{\gamma}$, then $\dot{Y}_\gamma = -k_\gamma\tilde{\gamma}^2 + \tilde{\gamma}\tilde{\theta}$.

Thirdly, design Q_r to make $\theta \rightarrow \theta_r$. Because

$$\begin{aligned}\dot{\tilde{\theta}} &= Q - \dot{\theta}_r \\ &= Q + \dot{\tilde{\delta}}_1 + k_\gamma\dot{\tilde{\gamma}} \\ &= Q + \tilde{\gamma} + k_\gamma\dot{\tilde{\gamma}} \\ &= Q + \tilde{\gamma} + k_\gamma(\theta + \Delta_\gamma)\end{aligned}\quad (21)$$

Let

$$Q_r = -k_\theta\tilde{\theta} - 2\tilde{\gamma} - k_\gamma(\theta + \hat{\delta}_2)\quad (22)$$

Then

$$\dot{\tilde{\theta}} = -k_\theta\tilde{\theta} - \tilde{\gamma} + \tilde{Q} + k_\gamma\tilde{\delta}_2\quad (23)$$

Select Lyapunov function

$$Y_\theta = \frac{1}{2}\tilde{\theta}^2 + \frac{1}{2b_\theta}\tilde{\delta}_2^2\quad (24)$$

Take the derivative of Y_θ

$$\begin{aligned}\dot{Y}_\theta &= \tilde{\theta}\dot{\tilde{\theta}} - \frac{1}{b_\theta}\tilde{\delta}_2\dot{\tilde{\delta}}_2 \\ &= \tilde{\theta}\left(-k_\theta\tilde{\theta} - \tilde{\gamma} + \tilde{Q} + k_\gamma\tilde{\delta}_2\right) - \frac{1}{b_\theta}\tilde{\delta}_2\dot{\tilde{\delta}}_2 \\ &= -k_\theta\tilde{\theta}^2 - \tilde{\gamma}\tilde{\theta} + \tilde{\theta}\tilde{Q} + \tilde{\delta}_2\left(k_\gamma\tilde{\theta} - \frac{1}{b_\theta}\dot{\tilde{\delta}}_2\right)\end{aligned}\quad (25)$$

Design adaptive law $\dot{\tilde{\delta}}_2 = k_\gamma b_\theta\tilde{\theta}$, then

$$\dot{Y}_\theta = -k_\theta\tilde{\theta}^2 - \tilde{\gamma}\tilde{\theta} + \tilde{\theta}\tilde{Q}\quad (26)$$

Finally, design control law of δ_e to make $Q \rightarrow Q_r$.

Because

$$\begin{aligned}\dot{\tilde{Q}} &= f_q + g_q\delta_e - \dot{Q}_r \\ &= f_q + g_q\delta_e + \left[k_\theta\tilde{\theta} + 2\tilde{\gamma} + k_\gamma(\theta + \hat{\delta}_2)\right]\end{aligned}\quad (27)$$

$$\begin{aligned}&= f_q + g_q\delta_e + k_\theta\dot{\tilde{\theta}} + 2\dot{\tilde{\gamma}} + k_\gamma\dot{\theta} + k_\gamma\dot{\hat{\delta}}_2 \\ &= f_q + g_q\delta_e + k_\theta(Q + \tilde{\gamma} + k_\gamma(\theta + \Delta_\gamma)) + 2(\theta + \Delta_\gamma) + k_\gamma Q + b_\theta k_\gamma^2\tilde{\theta} \\ &= f_q + g_q\delta_e + k_\theta Q + k_\theta\tilde{\gamma} + (2 + k_\gamma k_\theta)\theta + k_\gamma Q + b_\theta k_\gamma^2\tilde{\theta} + (2 + k_\gamma k_\theta)\Delta_\gamma\end{aligned}$$

Design

$$\begin{aligned}\delta_e &= g_q^{-1}\left[-k_\theta\tilde{Q} - f_q - k_\theta Q - k_\theta\tilde{\gamma} - (2 + k_\gamma k_\theta)\theta\right. \\ &\quad \left.- k_\gamma Q - b_\theta k_\gamma^2\tilde{\theta} - \tilde{\theta} - (2 + k_\gamma k_\theta)\hat{\delta}_2\right]\end{aligned}\quad (28)$$

Then

$$\dot{\tilde{Q}} = -k_\theta\tilde{Q} - \tilde{\theta} + (2 + k_\gamma k_\theta)\tilde{\delta}_3\quad (29)$$

Select Lyapunov function

$$Y_q = \frac{1}{2}\tilde{Q}^2 + \frac{1}{2b_q}\tilde{\delta}_3^2\quad (30)$$

Take the derivative of Y_q

$$\begin{aligned}\dot{Y}_q &= \tilde{Q}\dot{\tilde{Q}} - \frac{1}{b_q}\tilde{\delta}_3\dot{\tilde{\delta}}_3 \\ &= \tilde{Q}\left(-k_\theta\tilde{Q} - \tilde{\theta} + (2 + k_\gamma k_\theta)\tilde{\delta}_3\right) - \frac{1}{b_q}\tilde{\delta}_3\dot{\tilde{\delta}}_3 \\ &= -k_\theta\tilde{Q}^2 - \tilde{\theta}\tilde{Q} + \left((2 + k_\gamma k_\theta)\tilde{Q} - \frac{1}{b_q}\dot{\tilde{\delta}}_3\right)\tilde{\delta}_3\end{aligned}\quad (31)$$

Design adaptive law

$$\dot{\tilde{\delta}}_3 = b_q(2 + k_\gamma k_\theta)\tilde{Q}\quad (32)$$

Then

$$\dot{Y}_q = -k_\theta\tilde{Q}^2 - \tilde{\theta}\tilde{Q}\quad (33)$$

Now select Lyapunov function of the whole altitude loop $Y = Y_h + Y_\gamma + Y_\theta + Y_q$. Take the derivative of Y

$$\begin{aligned}\dot{Y} &= \dot{Y}_h + \dot{Y}_\gamma + \dot{Y}_\theta + \dot{Y}_q \\ &= -k_\gamma\tilde{\gamma}^2 + (-k_\gamma\tilde{\gamma}^2 + \tilde{\gamma}\tilde{\theta}) + (-k_\theta\tilde{\theta}^2 - \tilde{\gamma}\tilde{\theta} + \tilde{\theta}\tilde{Q}) \\ &\quad + (-k_\theta\tilde{Q}^2 - \tilde{\theta}\tilde{Q}) \\ &= -k_\gamma\tilde{\gamma}^2 - k_\theta\tilde{\theta}^2 - k_\theta\tilde{Q}^2 \leq 0\end{aligned}\quad (34)$$

So the altitude loop is stable.

4 Simulation

4.1 Maneuver Simulation

The maneuver trajectory is designed as: In the first 100s, the vehicle flies at 80000ft height with the speed of 8000ft/s, then in the next 300s, velocity increases to 10000ft/s and altitude goes up to 100000ft. Velocity climbs in a constant rate while parabola inserts in two ends to ensure smooth change as shown in (35)(36), and altitude climbs in a sinusoidal trajectory as shown in (37)(38).

Define

$$f_v(t) = \begin{cases} 0 & , 0 \leq t \leq t_{start} \\ \frac{1}{20t_{last} - 200}(t - t_{start})^2 & , t_{start} \leq t \leq t_{start} + 10 \\ \frac{1}{t_{last} - 10}(t - t_{start} - 5) & , t_{start} + 10 \leq t \leq t_{start} + t_{last} - 10 \\ 1 - \frac{1}{20t_{last} - 200}(t - t_{last} - t_{start})^2 & , t_{start} + t_{last} - 10 \leq t \leq t_{start} + t_{last} \\ 1 & , t \geq t_{start} + t_{last} \end{cases}\quad (35)$$

Then velocity reference is given by

$$V_{ref}(t) = V_0 + \Delta V * f_v(t)\quad (36)$$

Define

$$f_h(t) = \begin{cases} 0 & , 0 \leq t \leq t_{start} \\ -\frac{1}{2\pi} \cos\left(\frac{2\pi}{t_{last}}(t - t_{start}) - \frac{\pi}{2}\right) + \frac{(t - t_{start})}{t_{last}} & , t_{start} \leq t \leq t_{start} + t_{last} \\ 1 & , t \geq t_{start} + t_{last} \end{cases}\quad (37)$$

Then altitude reference is given by

$$h_{ref}(t) = h_0 + \Delta h * f_h(t)\quad (38)$$

The simulation results are shown in Fig 1, Fig 2.

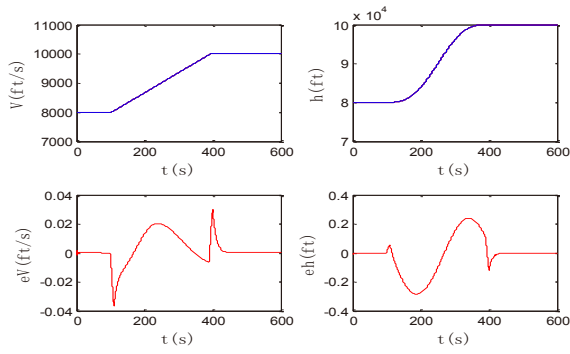


Fig. 1: Tracking graphs of velocity and altitude

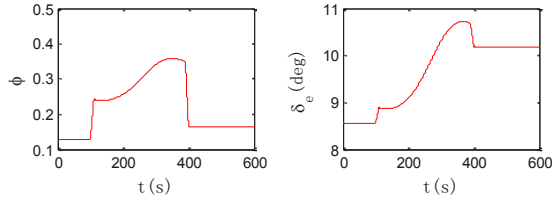


Fig. 2: Inputs Graphs

Fig 1 shows the tracking trajectories of velocity and altitude on the top and their tracking error below. It can be seen from Fig 1 that both velocity and altitude are tracked well, the tracking error is very small and turns to zero when outputs are steady. Fig 2 shows the value of inputs throughout the maneuver process, from which we can see that the inputs both vary smoothly without chattering.

4.2 Monte-Carlo Test

In fact, there may exist various uncertainties in the control object, thus robustness is quite required for the control system. Monte-Carlo method is an important tool in many assessments of the reliability and robustness of systems, structures or solutions. A Monte-Carlo test is usually carried out as follows:

- ① Define a domain of possible inputs.
- ② Generate inputs randomly from a probability distribution over the domain.
- ③ Perform a deterministic computation on the inputs.
- ④ Aggregate the results.

To evaluate the robustness of the controller, a monte-carlo test is carried, with 63 parameters of uncertainties are considered as show in table 5.

Table 5: Uncertain parameters of hypersonic vehicle

Vehicle Parameters	S, \bar{c}, m, I_{yy}
Lift Coefficients	$C_L^\alpha, C_L^{\delta_e}, C_L^0, C_L^{\eta_1}, C_L^{\eta_2}, C_L^{\eta_3}$
Drag Coefficients	$C_D^{\alpha^2}, C_D^\alpha, C_D^{\delta_e^2}, C_D^{\delta_e}, C_D^0, C_D^{\eta_1}, C_D^{\eta_2}, C_D^{\eta_3}$
Thrust Coefficients	$C_T^{\phi\alpha^3}, C_T^{\phi\alpha^2}, C_T^{\phi\alpha}, C_T^\phi, C_T^3, C_T^2, C_T^1, C_T^0, C_T^{\eta_1}, C_T^{\eta_2}, C_T^{\eta_3}$

Pitch Moment Coefficients	$C_M^{\alpha^2}, C_M^\alpha, C_M^0, C_M^{\delta_e}, C_M^{\eta_1}, C_M^{\eta_2}, C_M^{\eta_3}$
Generalized Forces Coefficients	$N_1^{\alpha^2}, N_1^\alpha, N_1^0, N_1^{\delta_e}, N_1^{\eta_1}, N_1^{\eta_2}, N_1^{\eta_3}$ $N_2^{\alpha^2}, N_2^\alpha, N_2^0, N_2^{\delta_e}, N_2^{\eta_1}, N_2^{\eta_2}, N_2^{\eta_3}$ $N_3^{\alpha^2}, N_3^\alpha, N_3^0, N_3^{\delta_e}, N_3^{\eta_1}, N_3^{\eta_2}, N_3^{\eta_3}$
Other Parameters	$z_T, \rho_0, g, \omega_1, \omega_2, \omega_3$

Suppose all parameters upon vary in $\pm 10\%$ range of their nominal value. Select uniform distribution to carry monte-carlo test. Take 1000 simulations which let the vehicle flies at 80000ft height with the speed of 8000ft/s. The results are showed in figure 3.

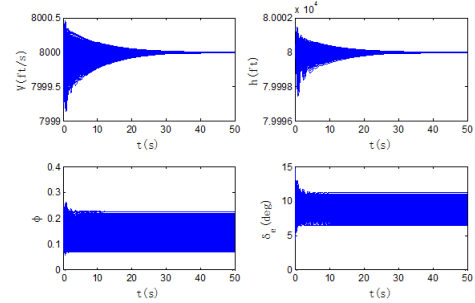


Fig. 3: Monte-Carlo test results

In Fig 3, the tracking trajectories of velocity and altitude are showed on the top and the value of inputs are showed below. It can be seen from Fig 3 that the output tracking error remains tiny and converges to zero throughout the 1000 simulations. It is thus clear that the controller proposed here can maintain a stable flight regardless of some uncertainties.

5 Conclusion

The original model of air-breathing hypersonic vehicle exhibits non-minimum phase which prevents the applicability of standard inversion methods for control design. A useful way to solve the non-minimum phase problem is control-oriented modeling, as which determines the process of control design in some degree. As it is verified that controller based on a proper control-oriented model can stabilize the origin model with non-minimum phase.

A simple control-oriented model with approximate integral chain altitude loop is developed in this paper, thus backstepping method can be conveniently used in control design. Model uncertainties are dealt with by adaptive control, whereas Lyapunov theory is employed for stability analysis. Simulations of maneuvering and robustness have been conducted on the original vehicle model. Although the system is stable as shown in the simulation results, stability analysis of the flexible states has not been studied which can be conducted in the future.

References

- [1] Voland R T, Huebner L D, McClinton C R. X-43A hypersonic vehicle technology development[J]. Acta Astronautica, 2006, 59(1): 181-191.
- [2] McClinton C R, Rausch V L, Nguyen L T, et al. Preliminary X-43 flight test results[J]. Acta Astronautica, 2005, 57(2): 266-276.

- [3] Parker J T, Serrani A, Yurkovich S, et al. Control-oriented modeling of an air-breathing hypersonic vehicle[J]. *Journal of Guidance, Control, and Dynamics*, 2007, 30(3): 856-869.
- [4] Sigthorsson D O. Control-oriented modeling and output feedback control of hypersonic air-breathing vehicles[D]. The Ohio State University, 2008.
- [5] Fiorentini L. Nonlinear adaptive controller design for air-breathing hypersonic vehicles[D]. The Ohio State University, 2010.
- [6] Rehman O U, Petersen I R, Fidan B. Robust nonlinear control design of a hypersonic flight vehicle using minimax linear quadratic Gaussian control[C]//*Decision and Control (CDC), 2010 49th IEEE Conference on. IEEE*, 2010: 6219-6224.
- [7] Rehman O U, Petersen I R, Fidan B. Robust nonlinear control of a nonlinear uncertain system with input coupling and its application to hypersonic flight vehicles[C]//*Control Applications (CCA), 2010 IEEE International Conference on. IEEE*, 2010: 1451-1457.
- [8] Rehman O U, Petersen I R, Fidan B. Feedback linearization-based robust nonlinear control design for hypersonic flight vehicles[J]. *Proceedings of the Institution of Mechanical Engineers, Part I: Journal of Systems and Control Engineering*, 2013, 227(1): 3-11.
- [9] Gao G, Wang J. Reference command tracking control for an air-breathing hypersonic vehicle with parametric uncertainties[J]. *Journal of the Franklin Institute*, 2013, 350(5): 1155-1188.
- [10] Zong Q, Wang J, Tao Y. Adaptive high - order dynamic sliding mode control for a flexible air - breathing hypersonic vehicle[J]. *International Journal of Robust and Nonlinear Control*, 2013, 23(15): 1718-1736.
- [11] Zong Q, Wang J, Tian B, et al. Quasi-continuous high-order sliding mode controller and observer design for flexible hypersonic vehicle[J]. *Aerospace Science and Technology*, 2013, 27(1): 127-137.
- [12] Wang J, Zong Q, Tian B, et al. Flight control for a flexible air-breathing hypersonic vehicle based on quasi-continuous high-order sliding mode[J]. *Systems Engineering and Electronics, Journal of*, 2013, 24(2): 288-295.
- [13] Tian B, Fan W, Zong Q, et al. Adaptive high order sliding mode controller design for hypersonic vehicle with flexible body dynamics[J]. *Mathematical Problems in Engineering*, 2013, 2013.
- [14] Fiorentini L, Serrani A. Nonlinear adaptive control design for non-minimum phase hypersonic vehicle models with minimal control authority[C]//*Decision and Control, 2009 held jointly with the 2009 28th Chinese Control Conference. CDC/CCC 2009. Proceedings of the 48th IEEE Conference on. IEEE*, 2009: 1405-1410.
- [15] Fiorentini L, Serrani A. Adaptive restricted trajectory tracking for a non-minimum phase hypersonic vehicle model[J]. *Automatica*, 2012, 48(7): 1248-1261.
- [16] Chaofang H, Lin W. Adaptive generalized backstepping control of hypersonic vehicles with integral filter[C]//*Control and Decision Conference (CCDC), 2012 24th Chinese. IEEE*, 2012: 2007-2011.
- [17] Xu B, Huang X, Wang D, et al. Dynamic surface control of constrained hypersonic flight models with parameter estimation and actuator compensation[J]. *Asian Journal of Control*, 2014, 16(1): 162-174.
- [18] Butt W A, Yan L, Kendrick A S. Adaptive dynamic surface control of a hypersonic flight vehicle with improved tracking[J]. *Asian Journal of Control*, 2013, 15(2): 594-605.
- [19] Zong Q, Wang F, Tian B, et al. Robust adaptive dynamic surface control design for a flexible air-breathing hypersonic vehicle with input constraints and uncertainty[J]. *Nonlinear Dynamics*, 2014, 78(1): 289-315.
- [20] Sigthorsson D, Jankovsky P, Serrani A, et al. Robust linear output feedback control of an airbreathing hypersonic vehicle[J]. *Journal of Guidance, Control, and Dynamics*, 2008, 31(4): 1052-1066.
- [21] Krstic M, Kanellakopoulos I, Kokotovic P V. *Nonlinear and adaptive control design*[M]. Wiley, 1995.